



## MR microneurography and quantitative T2 and DP measurements of the distal tibial nerve in CIDP

Paolo Florent Felisaz<sup>a,\*</sup>, Andrea Poli<sup>a</sup>, Raimondo Vitale<sup>a,b</sup>, Giovanni Vitale<sup>a,b</sup>, Carlo Asteggiano<sup>a,b</sup>, Niels Bergsland<sup>c</sup>, Ilaria Callegari<sup>d,e</sup>, Elisa Vegezzi<sup>d,e</sup>, Laura Piccolo<sup>d</sup>, Andrea Cortese<sup>d</sup>, Anna Pichiecchio<sup>a,f</sup>, Stefano Bastianello<sup>a,f</sup>

<sup>a</sup> Department of Neuroradiology, C. Mondino National Neurological Institute, Pavia, Italy

<sup>b</sup> Institute of Radiology, University of Pavia, Italy

<sup>c</sup> Buffalo Neuroimaging Analysis Center, Department of Neurology, Jacobs School of Medicine and Biomedical Sciences, University at Buffalo, The State University of New York, Buffalo, NY, USA

<sup>d</sup> Department of Neurology, C. Mondino National Neurological Institute, Pavia, Italy

<sup>e</sup> Neuroscience Consortium, University of Pavia, Monza Policlinico and Pavia Mondino, Italy

<sup>f</sup> Department of Brain and Behavioral Sciences, University of Pavia, Pavia, PV, Italy

### ARTICLE INFO

#### Keywords:

Neurography  
MRI  
Microneurography  
Micro  
CIDP  
Relaxometry  
Quantitative  
Nerve

### ABSTRACT

**Objective:** In this study we investigated the potential of magnetic resonance (MR) micro-neurography to detect morphological and relaxometric changes in distal tibial nerves in patients affected with chronic inflammatory demyelinating polyneuropathy (CIDP), and their associations with clinical and electrophysiological features.

**Materials and methods:** 10 subjects affected with CIDP and 10 healthy subjects were examined. Multiple MR parameters, including the number of fascicles (N), fascicles diameter (FD), total fascicles area (FA), epineurium area (EA), total nerve area (NA), fascicles to nerve ratio (FNR) and quantitative T2 and proton density (PD) were investigated on high resolution MR images of the distal tibial nerve. Those parameters were correlated with clinical scores, age of onset, disease duration and electrophysiologic data.

**Results:** Median NA and FA were significantly increased in the CIDP population (median values for NA in cm<sup>2</sup> in CIDP: 0.185; controls: 0.135; p: 0.028; for FA in CIDP 0.136; controls 0.094; p: 0.021). There was no correlation between the parameters investigated and clinical or electrophysiologic features.

**Conclusion:** MR microneurography can detect increased total nerve and fascicle area in distal tibial nerves in CIDP and may be useful for diagnosing CIDP.

### 1. Introduction

Chronic inflammatory demyelinating polyneuropathy (CIDP) is an acquired, immune-mediated inflammatory disorder causing demyelinating peripheral neuropathy with a slowly progressive or relapsing course.

The estimated prevalence is 8.9 per 100,000 people and although it is a rare medical condition, CIDP encompasses ca. 13% of all cases of neuropathy referred to neuromuscular clinics [1,2]. The diagnosis of CIDP is based on a multi-criteria algorithm, including clinical examination, nerve conduction studies (NCS), and cerebral spinal fluid

examination, but imaging techniques such as MRI and ultrasound (US) are increasingly used to support the diagnosis, assessment of the clinical course and response to treatment.

Typical findings in CIDP include nerve enlargement, T2 signal increase and enhancement of nerve roots, especially at the first stages of the disease [3]. Proximal nerve involvement is typical at the onset and becomes more prominent and ubiquitous in the long-term. Nerve enlargement is also positively correlated with disease duration [4–6]. However, correlation of MRI features with clinical disability or response to treatment is controversial [7] and reliable biomarkers of disease detection and progression are still lacking.

**Abbreviations:** MRI, magnetic resonance imaging; CIDP, chronic inflammatory demyelinating polyneuropathy; N, number of fascicles; FD, fascicles diameter; FA, total fascicles area; EA, epineurium area; NA, total nerve area; FNR, fascicles to nerve ratio; PD, proton density; NCS, nerve conduction studies; MRC-APF, Medical Research Council muscle strength score for Ankle Plantar Flexion of the imaged side; MRC-LL, Medical Research Council muscle strength sum score for the Lower Limbs; INCAT-LL, Inflammatory Neuropathy Cause and Treatment score for the Lower Limbs; ISS-LL, INCAT sensory score for the Lower Limbs

\* Corresponding author at: Neuroradiology department, C. Mondino Neurological National Institute, Università di Pavia, via Mondino 2, 27100 Pavia, Italy.

E-mail address: [paolo.felisaz@gmail.com](mailto:paolo.felisaz@gmail.com) (P.F. Felisaz).

<https://doi.org/10.1016/j.jns.2019.03.001>

Received 12 September 2018; Received in revised form 10 February 2019; Accepted 4 March 2019

Available online 11 March 2019

0022-510X/ © 2019 Elsevier B.V. All rights reserved.

Most previous works on MRI of CIDP were focused on the spinal nerve roots and proximal nerve trunks, and there is a paucity of works on the distal involvement of nerves [8]. The extremities can be imaged with smaller surface coils reaching greater resolution, allowing direct visualization of nerve ultrastructure. In previous studies, we have shown the possibility to visualize the tibial nerve at the ankle with microscopic resolution, using a standard clinical set of MRI hardware and sequences [9–11]. With these techniques, in plane resolution up to 100  $\mu\text{m}$  can be reached allowing direct visualization of the nerve fascicles, the epineurium, the perineurium and fat infiltration.

In this study we evaluated the role of MR micro-neurography in detecting morphological, structural and relaxometric changes in distal tibial nerves in patients affected with CIDP, and their correlation with clinical and electrophysiological features. In particular, we investigated the diagnostic potential of morphologic features such as the number of fascicles (N), their mean diameter (FD), the total area of fascicles (FA), epineurium (EA), nerve (NA) and the fascicle to nerve area ratio (FNR), and quantitative relaxometric parameters such as T2 and proton density (PD).

## 2. Materials and methods

### 2.1. Subjects and clinical evaluation

This study was approved by our institutional review board and all subjects provided written informed consent. We included a convenience sample of 10 CIDP patients with variable disease and treatment duration who met the European Federation Society/Peripheral Nerve Society definite diagnostic criteria for CIDP [12]. Ten healthy subjects matched by sex and age were imaged as a control group. The controls were excluded if they had either clinical evidence or past history of lumbar roots compression, peripheral polyneuropathy, tarsal tunnel syndrome, diabetes mellitus, major trauma, or surgery at the lower limbs.

All patients were clinically examined at the time of MRI to assess the severity of the neuropathy and their overall disability. Muscle strength was scored using the Medical Research Council (MRC) grading scale [13] (grades 0–5: 5 = normal power, 4 = active movement against strength and resistance, 3 = active movement against gravity, 2 = active movement with gravity eliminated, 1 = flicker or trace contraction, 0 = no contraction), evaluated for ankle plantar flexion of the imaged side (MRC-APF) and the sum score of the lower limbs (MRC-LL; maximum score 30). Disability was graded using the Inflammatory Neuropathy Cause and Treatment (INCAT) disability sum score restricted only to the legs (INCAT-LL; grades 0–7, in brief: 0 = walking not affected, 1 = walking is affected but does not look abnormal, 2 = walks independently but gaits looks abnormal, 3 = needs unilateral support to walk 10 m, 4 = needs bilateral support to walk 10 m, 5 = needs wheelchair to travel 10 m, 6 = restricted to wheelchair, 7 = complete movement restriction) [14]. The INCAT sensory sum score (ISS) was used for grading the deficit of sensitivity for the lower limb imaged (ISS-LL; pinprick grade 0–4, vibration sense grade 0–4, total 0–8 with 0 = normal sensation and 8 = maximum sensory deficit).

NCS data from the tibial nerve imaged were available for all patients within a period  $\pm$  6 months from the MRI examination, including distal muscle action potential amplitudes and motor nerve conduction velocity.

### 2.2. Imaging technique

Examinations were performed on a 3 T MRI scanner (Discovery MR750 3.0 T scanner - GE Healthcare, Milwaukee) using a six-channel carotid coil adapted for the study of the ankle. The coil guarantees high signal-to-noise ratio (SNR) for superficial structures and can adapt to anatomical irregularities of the region under study. Imaging was

applied to the dominant leg of the patients and healthy controls.

The protocol included the following sequences:

- (1) 3D Localizer. 3D spoiled gradient echo (SPGR) sequence with fat saturation and isotropic voxels (TR: 5,9 ms, TE: 2,1 ms, FA: 10°, FOV: 8  $\times$  8 cm, matrix: 128  $\times$  128, 128 slices, thickness: 1 mm, time of scan: 1 min), a low-resolution 3D sequence aimed to visualize the neurovascular bundle of the tibial nerve, at the medial aspect of the tibia. The following sequences were oriented along a transverse plane perpendicular to the main axis of the tibial nerve, achieved with the multiplanar reconstruction on the 3D localizer. The top axial slice of each sequence was positioned at 5 cm above the tibial malleolus, measuring on the 3D localizer down to top from the point of maximum convexity of the malleolus.
- (2) 3D SPGR IDEAL. High-resolution fluid sensitive sequence obtained with IDEAL (Iterative Decomposition of water and fat with Echo Asymmetry and Least-squares estimation - GE Healthcare Milwaukee USA). IDEAL is based on a 3-point Dixon technique and provides images of water only, fat only, in phase and out of phase (TR: 16,9 ms, TE: 5,3 ms, FA: 10°, FOV: 6  $\times$  6 cm, matrix: 512  $\times$  420, 14 slices, thickness: 2 mm, time of scan: 6 min).
- (3) 2D fast spin echo (FSE) T1 weighted image (TR: 650 ms, TE: 10 ms, FA: 90°, FOV: 6  $\times$  6 cm, matrix: 512  $\times$  426, 14 slices, thickness: 2 mm, time of scan: 5 min).
- (4) Dual echo FSE used for signal quantification of T2 and PD of the tibial nerves (TR: 5000 ms, TE1 13 ms, TE2 75 ms, FOV: 15  $\times$  15 cm, matrix: 480  $\times$  480, 8 slices, thickness: 4 mm, time of scan: 8 min).

The total scan time was approximately of 30 min including the positioning of the subject on the scanner and the selection of the correct plane on the 3D localizer sequence.

### 2.3. Data analysis

Morphometric parameters (N, FD, NA, FA, EA and FNR) were obtained from the high-resolution Sequences (2) and (3). Signal quantification of T2 and proton density (PD) of the tibial nerves was obtained with Sequence (4).

Since the fascicles were not always perfectly visually separable, N was obtained counting the number of fascicles on three random slices on the Sequence (2) and (3) (for a total of 6 images) and calculating their mean. The mean FD was obtained with manual measurements on 10 random fascicles of one slice of Sequence (3), measuring the distance of two opposite points on the fascicle's rim passing through the center, and calculating their mean. NA, FA and EA, were obtained using the two-classes segmentation process described in a previous paper [10]. Briefly, the tibial nerve was manually outlined on each axial slice of the in-phase image using the software JIM (Xinapse Systems Ltd., Essex, UK). Then, the selected region of interest was processed with FAST (FMRIB's Automated Segmentation Tool, Analysis Group, Oxford, UK) [15] on the corresponding high resolution T1 image. Segmentation was performed with a two class Gaussian Mixture Model with Markov random field algorithm based on signal and spatial intensity variation, in order to obtain FA (corresponding to the dark pixels), EA (corresponding to the brighter pixels encompassing the fascicles) and NA for each slice (for a total of 14 slices). Overall, if the tibial nerve bifurcated within the acquired volume, both the main trunk and the secondary trunk(s) were considered with summation of the ROIs. The final values of FA, EA and NA consisted with the means of the areas measured on the 14 slices.

Quantitative signal measurements of T2 and PD were obtained by analyzing Sequence (4). Regions of interests of the tibial nerve were manually outlined on each axial slice of the TE1 image, then the mean signal intensities of the TE1 image and the corresponding TE2 image were computed with Eqs. (1) and (2) to obtain T2 and PD.

$$T2 = \frac{TE2 - TE1}{\ln(SI(TE1)/SI(TE2))} \tag{1}$$

$$PD = \frac{SI(TE1)}{1 - \frac{TE1}{T2}} \tag{2}$$

### 2.4. Statistical analysis

Statistical analyses were performed with MedCalc (MedCalc software, Ostend, Belgium).

Due to the small sample size non-parametric statistics were used. The Mann Whitney *U* test was used to compare T2, PD, N, FD, FA, EA, NA and FNR between patients and controls. Correlations of the MR parameters with the duration of the disease, age of onset, clinical scores and neurophysiologic parameters (in particular, the distal muscle action potential amplitudes and motor nerve conduction velocity of the tibial nerves) were tested with the Spearman's rank coefficient. *P* values lower than 0.05 were considered statistically significant.

### 3. Results

A total of 10 patients affected with CIDP were imaged (7 men and 3 women; age range 31–74, median 64 years). Detailed demographics of the patients are shown in Table 1. Mean age of onset was 54 years (range 10–74, SD 19.4), with an average disease duration at the time of the study of 8,8 years (range 1–20, SD 6.8). Median INCAT-LL disability score was 2 (range 0–3), median ISS-LL score 4.5 (range 2–8), median MRC-LL 30 (range 28–30); MRC-APF was maximum (5) for all patients. The clinical course was relapsing-remitting in 6/10 patients, chronic-progressive in 3/10 and monophasic in 1 patient. Relevant NCS data for the purpose of the study are reported in Table 1. 10 healthy subjects were included to serve as a control group (6 men and 4 women; Age range 30–76, median 65 years) Fig. 1.

The median FA and NA were significantly greater in the CIDP group compared to controls (Table 2, Fig. 2). The median FD was also greater in the CIDP group without reaching statistical significance (the *p* values were slightly above the limit value with *p* = 0.069). There were no significant differences between the two groups for N, mean EA and FNR. There was no significant difference in T2 and PD values between the two groups.

We found no correlations between any of the parameters in the study and age of onset, disease duration, MRC-APF, MRC-LL, INCAT-LL and ISS-LL scores or the NCS parameters.

### 4. Discussion

In this study we investigated the diagnostic potential of MR micro-neurography, a novel technique capable to assess the ultrastructure of nerves, in distinguishing patients affected with CIDP and normal subjects. Multiple morphological and relaxometric parameters were assessed and correlations with clinical features and disease severity were explored. We have found significant increases in total NA and FA in CIDP patients, however, none of the parameters investigated was significantly correlated to duration of the disease, age of onset, disease severity or electrophysiological data.

Nerve roots and proximal nerve enlargement is a common finding in patients affected with CIDP and it has been well demonstrated both with MRI and US [4–6,8,16–19], and our results are in line and complement the previous literature indicating that nerve hypertrophy also occurs at the distal tibial nerve tract of the leg. We have shown also significant FA increase in CIDP patients, in contrast with a stable epineurial area, suggesting that the cause of nerve enlargement is the net increase of FA. The FD was also increased (without statistical significance although the *p*-value was very close to the limit of 0.05) while as expected, the FNR and N were not different between the two groups.

**Table 1**  
Demographics and clinical information of the population. MRC-APF (MRC muscle strength score for ankle plantar flexion) is referred to the leg imaged, (the dominant). MRC-LL (MRC muscle strength sum score), ISS-LL (INCAT sensory score) and INCAT-LL (INCAT disability score) are referred to the inferior limbs only. For the EMG data, distal muscle action potential amplitudes (AMP) and motor nerve conduction velocities (CV) of the tibial nerve imaged are reported.

	Age	Sex	Age of onset	Disease duration	First line treatment	Actual treatment	Diagnosis EFNS	Course	MRC-APF	MRC-LL	ISS-LL	INCAT-LL	AMP TP (mV)	CV TP (m/s)
1	54	F	36	18	Steroid, Ivig	Ivig	Typical definite	Relapsing	5	30	4	2	2.8	18.3
2	76	M	73	3	Steroid	Ivig	Typical definite	Relapsing	5	30	1	1	3.6	37.5
3	72	M	63	9	Ivig	Steroid	Atypical definite	Relapsing	5	30	4	0	7.5	30.8
4	30	M	10	20	Steroid, Azathioprin	Steroid + Ivig	Typical definite	Progressive	5	28	4	2	0.2	22.2
5	61	M	60	1	Steroid	Steroid	Atypical definite	Relapsing	5	30	5	1	0.2	13.5
6	74	F	65	9	Azathioprin	Azathioprin	Typical definite	Progressive	5	30	5	2	1.4	37.6
7	75	M	74	1	Ivig	Ivig	Typical definite	Monophasic	5	30	2	2	0.5	22.2
8	59	M	47	12	Steroid then Ivig, PEX, cyclofosamide)	Steroid	Typical definite	Progressive	5	30	2	3	1.3	30.4
9	47	F	44	3	PEX	no	Typical definite	Relapsing	5	30	1	0	8.5	33.2
10	70	M	58	12	Ivig	no	Typical definite	Relapsing	5	30	6	2	2.1	33.8

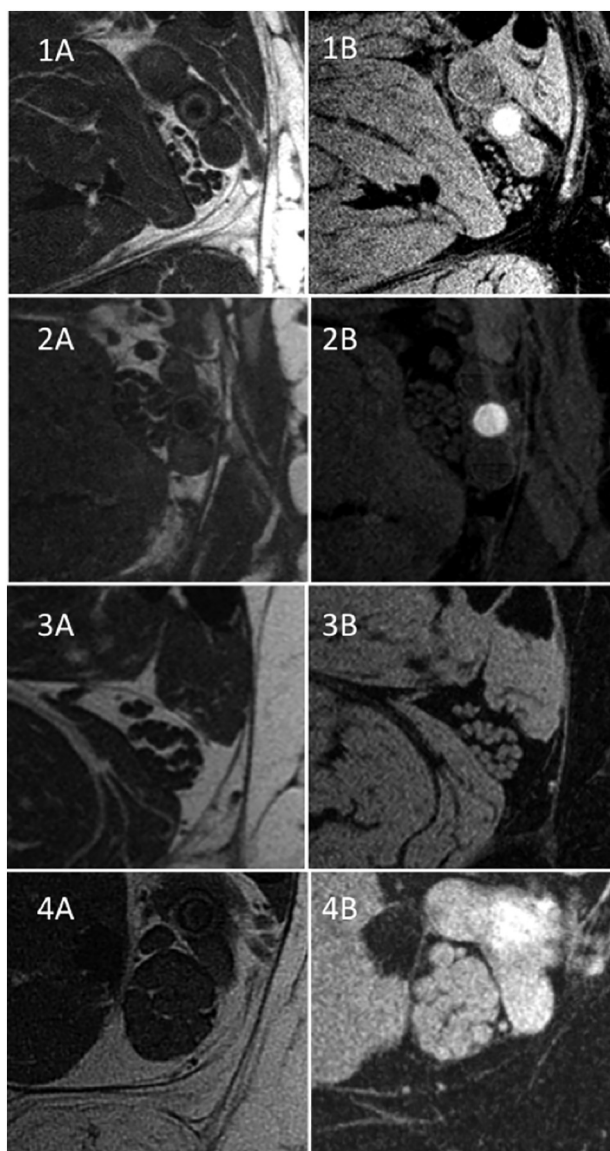


**Fig. 1.** Examples of the distal tibial nerve images. Images on the left are T1 weighted (see Sequence (3) in the text), on the right high-resolution 3D SPGR IDEAL (see Sequence (2) in the text). [1,2] Tibial nerves from control subjects and [3,4] from patients affected with CIDP. On patient 4 the fascicles are remarkably enlarged, though this subject had intermediate clinical score (see discussion).

Nevertheless, the relationship between the degree of nerve hypertrophy and disability remains unclear. Even after removing the most extreme value of NA, FA and FD, no statistical significance was reached for correlations with clinical features. It has been shown that nerve enlargement is positively correlated with disease duration [4,6] and electrophysiological parameters [8]. However there is no evidence that it is correlated with disease activity or severity [5,8,16], nor to treatment response [7]. Similarly to our study, Pitarokoli et al. [19] demonstrated nerve fascicles swelling in subjects with a moderate grade of neuropathy, assessed in a qualitative manner. Interestingly, they reported two cases of fascicles atrophy and increase of intraneural fat, occurring in subjects with the higher grade of disability. However, because of the small number of cases, the relationship between fascicles hypertrophy during disease activity and atrophy in the later stages could not be established.

T2-weighted nerve hyperintensity is also a common finding in CIDP patients, especially at the first stages of the disease [16], and it has been

**Table 2**  
Median values of the parameters considered in the study: T2 and PD, number of fascicles (N), fascicles diameter (FD), total fascicles area (FA), epineurium area (EA) total nerve area (NA) and fascicles to nerve ratio (FNR). Significant differences between the two groups are present for FA and NA. FD is at the limit of statistical significance.

	T2 (ms)	DP	N	FD (µm)	FA (cm <sup>2</sup> )	EA (cm <sup>2</sup> )	NA (cm <sup>2</sup> )	FNR
Controls	55.7 (29.6–93.6)	3898 (588–6133)	22.5 (19–27)	446.5 (398–492)	0.094 (0.065–0.131)	0.035 (0.014–0.071)	0.135 (0.099–0.169)	0.713 (0.580–0.873)
CIDP	52.8 (31.8–81.3)	5256 (1399–9206)	21.5 (17–25)	543.6 (382–1006)	0.136 (0.069–0.337)	0.040 (0.022–0.085)	0.185 (0.103–0.359)	0.7201 (0.600–0.939)
P	0.850	0.315	0.425	0.069	0.021	0.241	0.028	0.630

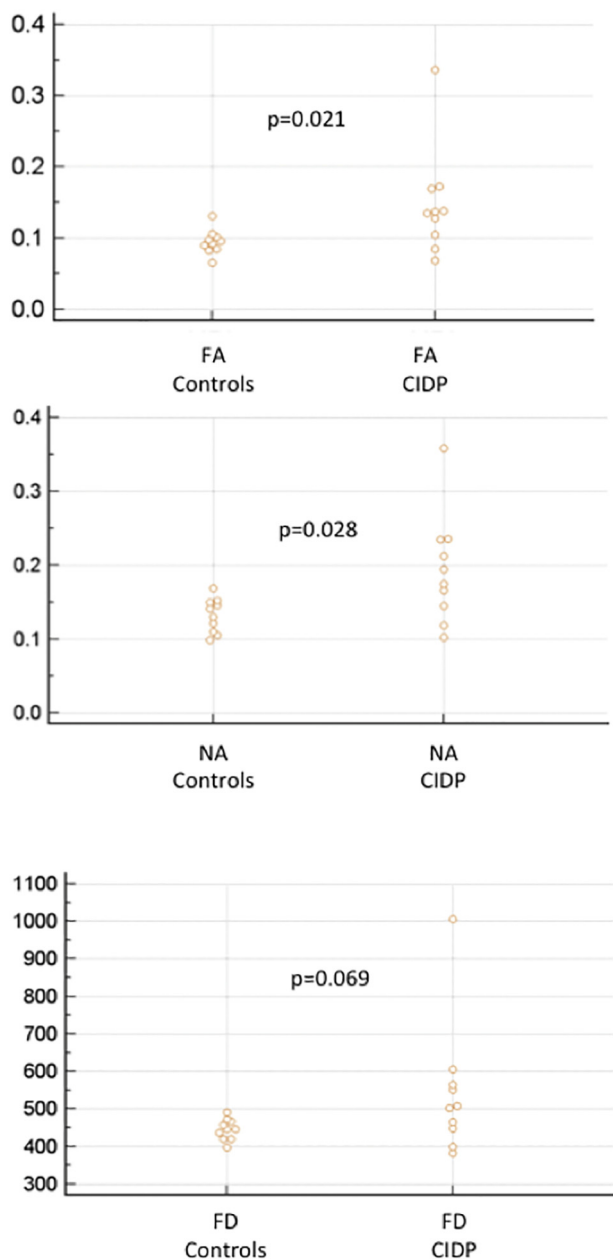


Fig. 2. Values of total fascicles area (FA), total nerve area (NA) and fascicles diameter (FD) for control subjects and CIDP patients are graphically represented. Statistically significant differences are present for FA and NA.

quantitatively demonstrated as an increase of proton density [8]. Though it is typical at the nerve roots and the proximal tract of the sciatic nerve, it has not been described at the distal nerve tracts yet. In our study that focused on the distal tracts of the tibial nerve, we did not find significant differences in T2 and PD. Nevertheless, as in the case of nerve area, there are no clinical correlations known for signal intensity of the nerve.

Other MR parameters have also been investigated and associated with the presence of the disease, such as fractional anisotropy, fat fraction of the innervated muscles, and nerve roots contrast enhancement but, in a similar way, none of them showed correlations with disease activity or severity [5,16,17]. At this stage we can conclude that, even if MRI can help in differentiating subjects affected with CIDP, it is not a reliable biomarker of CIDP that could be used for assessing disease progression or response to treatment. There are some limitations in previous studies. However, the main one, shared by ours, is the

constantly small sample of patients that reduces the power to separate different grades of severity and to detect correlations between MR parameters and clinical features. The other question is whether those MR parameters investigated so far (nerve diameter, overall nerve signal, etc.) can effectively reflect the pathophysiological changes occurring within the affected nerves. It can be argued that internal nerve components, which include both neural (fascicles) and connective tissue (epineurium, perineurium, endoneurium), may contribute concurrently to the total nerve diameter. For example, in diabetic neuropathy, the NA increases as well, but as a result of the increase of the EA and not FA. It is likewise unclear what is the pathological basis of the increase of nerve signal in T2 weighted images, a feature shared with other neuropathies, such as amyloid and diabetic forms [20–22]. The primary effort of our study was to provide new MR parameters that may more specifically reflect alterations occurring within nerves, giving new insights over the pathology of the disease. Pathological findings in nerves affected with CIDP include subepineurial edema, inflammation, axonal changes, onion bulb formation, but the key neuropathological feature is the unequivocal demonstration of demyelination that requires teased fibers preparation and electron microscopy [23–26]. None of these features is visible with MRI performed with standard clinical equipment anyway as of now. Nevertheless, our method can non-invasively show some additional information about the neural and connective neural tissues, which may reflect the alterations in nerve caliber or overall nerve signal.

This study has some limitations. As mentioned above, the sample size was rather small, owing to the rarity of the disorder; hence the lack of correlations with clinical disability should be interpreted cautiously. Furthermore, our cohort included only subjects with mild to moderate grades of disability, with INCAT-LL maximum 3 and preserved muscular function (the MRC-APF and MRC-LL were almost always normal). Thus, we could not expect to demonstrate that our method is a specific biomarker of the disease, however, the fact that patients with mild grade disability have significant alterations in MR parameters strengthens the possible role of our method in the diagnostic process of the disease. For reasons of scanning time we focused our examination on a single leg and we arbitrarily decided to image the dominant one, as we assumed symmetry of the nerve lesions, but asymmetrical patterns are possible. In other previous studies a single leg was studied as well, either the more affected or systematically the same side [6,17]. The choice of the side is a matter of discussion but imaging both legs is possibly the best choice. Moreover, we have taken measurements for only a small tract of the nerve at the distal leg, which may not be representative of the whole nerve involvement of the disease. The main advantage of our protocol remains the in-plane resolution that allowed for counting the single fascicles and measuring their diameter. True transverse sections and measures of the nerves areas components were also provided, in contrast to pure axial slices that may crosscut the nerves in their oblique tracts.

In conclusion this study confirmed an increase of nerve area in subjects affected with CIDP at the distal tibial nerve, in agreement with the previously described increase in nerve area on more proximal locations of the sciatic nerve. This increase of NA is a consequence of the increase of the FA, as shown with the MR micro-neurography technique. However, none of the morphological or relaxometric parameters that we investigated were strongly correlated to clinical or electrophysiological gravity, thus they should not be considered as biomarkers of the disease. The role of MRI in the diagnostic and guiding treatment in patients with CIDP still needs further validation and prospective clinical studies with larger cohorts are warranted to generate more robust data.

#### Conflict of interest disclosure

On behalf of all authors, the corresponding author states that there is no conflict of interest.

## References

- [1] R. Hadden, European federation of neurological societies/peripheral nerve society guideline \* on management of paraproteinemic demyelinating neuropathies. Report of a joint task force of the European federation of neurological societies and the peripheral nerve society-first revision, *J. Peripher. Nerv. Syst.* (2010), <https://doi.org/10.1111/j.1529-8027.2010.00278.x>.
- [2] H. Köller, B.C. Kieseier, S. Jander, H.-P. Hartung, Chronic inflammatory demyelinating polyneuropathy, *N. Engl. J. Med.* (2005), <https://doi.org/10.1056/NEJMra041347>.
- [3] S.K. Thawait, V. Chaudhry, G.K. Thawait, K.C. Wang, A. Belzberg, J.A. Carrino, A. Chhabra, High-resolution MR neurography of diffuse peripheral nerve lesions, *Am. J. Neuroradiol.* (2011), <https://doi.org/10.3174/ajnr.A2257>.
- [4] T. Ishikawa, K. Asakura, Y. Mizutani, A. Ueda, K.I. Murate, C. Hikichi, S. Shima, M. Kizawa, M. Komori, K. Murayama, H. Toyama, S. Ito, T. Mutoh, MR neurography for the evaluation of CIDP, *Muscle Nerve* (2017), <https://doi.org/10.1002/mus.25368>.
- [5] G. Midroni, L.N. De Tilly, B. Gray, J. Vajsar, MRI of the cauda equina in CIDP: clinical correlations, *J. Neurol. Sci.* (1999), [https://doi.org/10.1016/S0022-510X\(99\)00195-1](https://doi.org/10.1016/S0022-510X(99)00195-1).
- [6] C.D.J. Sinclair, M.A. Miranda, P. Cowley, J.M. Morrow, I. Davagnanam, H. Mehta, M.G. Hanna, M. Koltzenburg, M.M. Reilly, T.A. Yousry, J.S. Thornton, MRI shows increased sciatic nerve cross sectional area in inherited and inflammatory neuropathies, *J. Neurol. Neurosurg. Psychiatry* (2011), <https://doi.org/10.1136/jnnp.2010.211334>.
- [7] B.A. Jongbloed, J.W. Bos, D. Rutgers, W.L. van der Pol, L.H. van den Berg, Brachial plexus magnetic resonance imaging differentiates between inflammatory neuropathies and does not predict disease course, *Brain Behav.* (2017), <https://doi.org/10.1002/brb3.632>.
- [8] M. Kronlage, P. Bäumer, K. Pitarokoiili, D. Schwarz, V. Schwehr, T. Godel, S. Heiland, R. Gold, M. Bendszus, M.S. Yoon, Large coverage MR neurography in CIDP: diagnostic accuracy and electrophysiological correlation, *J. Neurol.* (2017), <https://doi.org/10.1007/s00415-017-8543-7>.
- [9] P.F. Felisaz, E.Y. Chang, I. Carne, S. Montagna, F. Balducci, G. Maugeri, A. Pichiechio, F. Calliada, M. Baldi, S. Bastianello, In vivo MR microneurography of the tibial and common peroneal nerves, *Radiol. Res. Pr.* 2014 (2014) 780964, <https://doi.org/10.1155/2014/780964>.
- [10] P.F. Felisaz, F. Balducci, S. Gitto, I. Carne, S. Montagna, R. De Icco, A. Pichiechio, M. Baldi, F. Calliada, S. Bastianello, Nerve fascicles and epineurium volume segmentation of peripheral nerve using magnetic resonance micro-neurography, *Acad. Radiol.* (2016), <https://doi.org/10.1016/j.acra.2016.03.013>.
- [11] P.F. Felisaz, G. Maugeri, V. Busi, R. Vitale, F. Balducci, S. Gitto, P. Leporati, A. Pichiechio, M. Baldi, F. Calliada, L. Chiovato, S. Bastianello, MR micro-neurography and a segmentation protocol applied to diabetic neuropathy, *Radiol. Res. Pract.* (2017), <https://doi.org/10.1155/2017/2761818>.
- [12] P.Y.K. Van den Bergh, R.D.M. Hadden, P. Bouche, D.R. Cornblath, A. Hahn, I. Illa, C.L. Koski, J.-M. Léger, E. Nobile-Orazio, J. Pollard, C. Sommer, P.A. van Doorn, I.N. van Schaik, European federation of neurological societies/peripheral nerve society guideline on management of chronic inflammatory demyelinating polyradiculoneuropathy, *Eur. J. Neurol.* (2010), <https://doi.org/10.1111/j.1468-1331.2009.02930.x>.
- [13] G. Riddoch, Medical Research Council. Aids to the Examination of the Peripheral Nervous System, Memo. No. 45, Her Majesty's Station. Off, London, 1975, <https://doi.org/10.1212/WNL.38.10.1663-a>.
- [14] I.S.J. Merkies, P.I.M. Schmitz, F.G.A. Van der Meché, J.P.A. Samijn, P.A. Van Doorn, Inflammatory neuropathy cause, clinimetric evaluation of a new overall disability scale in immune mediated polyneuropathies, *J. Neurol. Neurosurg. Psychiatry* (2002), <https://doi.org/10.1136/jnnp.72.5.596>.
- [15] Y. Zhang, M. Brady, S. Smith, Segmentation of brain MR images through a hidden Markov random field model and the expectation-maximization algorithm, *IEEE Trans. Med. Imaging* (2001), <https://doi.org/10.1109/42.906424>.
- [16] A.J. Duggins, J.G. McLeod, J.D. Pollard, L. Davies, F. Yang, E.O. Thompson, J.R. Soper, Spinal root and plexus hypertrophy in chronic inflammatory demyelinating polyneuropathy, *Brain.* (1999), <https://doi.org/10.1093/brain/122.7.1383>.
- [17] T. Lichtenstein, A. Sprenger, K. Weiss, K. Slebocki, B. Cervantes, D. Karampinos, D. Maintz, G.R. Fink, T.D. Henning, H.C. Lehmann, MRI biomarkers of proximal nerve injury in CIDP, *Ann. Clin. Transl. Neurol.* (2018), <https://doi.org/10.1002/acn3.502>.
- [18] P. Lozeron, M.C. Lacour, C. Vandendries, M. Théaudin, C. Cauquil, C. Denier, C. Lacroix, D. Adams, Contribution of plexus MRI in the diagnosis of atypical chronic inflammatory demyelinating polyneuropathies, *J. Neurol. Sci.* (2016), <https://doi.org/10.1016/j.jns.2015.11.048>.
- [19] K. Pitarokoiili, M. Schlamann, A. Kerasnoudis, R. Gold, M.S. Yoon, Comparison of clinical, electrophysiological, sonographic and MRI features in CIDP, *J. Neurol. Sci.* (2015), <https://doi.org/10.1016/j.jns.2015.07.030>.
- [20] M. Pham, D. Oikonomou, B. Hornung, M. Weiler, S. Heiland, P. Bäumer, J. Kollmer, P.P. Nawroth, M. Bendszus, Magnetic resonance neurography detects diabetic neuropathy early and with proximal predominance, *Ann. Neurol.* 78 (2015) 939–948.
- [21] J. Kollmer, E. Hund, B. Hornung, U. Hegenbart, S.O. Schonland, C. Kimmich, A.V. Kristen, J. Purrucker, C. Rocken, S. Heiland, M. Bendszus, M. Pham, In vivo detection of nerve injury in familial amyloid polyneuropathy by magnetic resonance neurography, *Brain* (2014), <https://doi.org/10.1093/brain/awu344>.
- [22] J. Kollmer, M. Bendszus, M. Pham, MR neurography: diagnostic imaging in the PNS, *Clin. Neuroradiol.* 25 (Suppl. 2) (2015) 283–289, <https://doi.org/10.1007/s00062-015-0412-0>.
- [23] M. Nagamatsu, S. Terao, K. Misu, M. Li, N. Hattori, M. Ichimura, M. Sakai, H. Yamamoto, H. Watanabe, S. Riku, E. Ikeda, J. Hata, M. Oda, M. Satake, N. Nakamura, S. Matsuya, Y. Hashizume, G. Sobue, Axonal and perikaryal involvement in chronic inflammatory demyelinating polyneuropathy, *J. Neurol. Neurosurg. Psychiatry* (1999), <https://doi.org/10.1136/jnnp.66.6.727>.
- [24] E.K. Mathey, S.B. Park, R. a C. Hughes, J.D. Pollard, P.J. Armati, M.H. Barnett, B.V. Taylor, P.J.B. Dyck, M.C. Kiernan, C.S.-Y. Lin, Chronic inflammatory demyelinating polyradiculoneuropathy: from pathology to phenotype, *J. Neurol. Neurosurg. Psychiatry* (2015), <https://doi.org/10.1136/jnnp-2014-309697>.
- [25] A. Taly, A. Nalini, S. Shankar, A. Mahadevan, G. Kulkarni, Sural nerve biopsy in chronic inflammatory demyelinating polyneuropathy: are supportive pathologic criteria useful in diagnosis? *Neurol. India* (2010), <https://doi.org/10.4103/0028-3886.68673>.
- [26] D.S. Molenaar, M. Vermeulen, R. de Haan, Diagnostic value of sural nerve biopsy in chronic inflammatory demyelinating polyneuropathy, *J. Neurol. Neurosurg. Psychiatry* (1998), <https://doi.org/10.1136/jnnp.64.1.84>.